

Comparative Study of Amplification Factors for Different Earthquake Scenarios in Kathmandu Valley

Saroj Prasad Adhikari ^a, Ram Chandra Tiwari ^b, Khemraj Pokhrel ^c

^a Department of Civil Engineering, Pulchowk Campus, IOE, Tribhuvan University, Nepal

✉ ^a adhikarisaroj77@gmail.com, ^b rctiwari1975@gmail.com, ^c khemrajpokhrel207@gmail.com

Abstract

Seismicity is a significant concern in Nepal, particularly in the complex geological and geotechnical setting of the Kathmandu valley. This study presents a comprehensive site-specific response analysis of the Kathmandu valley using DEEPSOIL software for non-linear one-dimensional analysis. The primary focus is on evaluating the impact of five distinct earthquake motions: the Gorkha Earthquake motion, the Loma Gilroy Earthquake motion, the Aftershocks of the Gorkha Earthquake motion, the Chi-Chi Earthquake motion, and the Kobe Earthquake motion. The study investigates whether the various locations of Kathmandu valley are amplified or de-amplified during the different earthquake motions. Notably, the results reveal higher Amplification factor values for the Gorkha Earthquake motion and its aftershocks compared to the rest of the earthquake motions. However, the Kobe Earthquake motion represents an exception, with significant amplification reduction. Among the regions studied, Balaju stands out with the highest ground motion amplification, attributed to the presence of layers of grey loose micaceous silty fine sand in its subsurface geology.

Keywords

Aftershocks, Amplification factor(AF), DEEPSOIL, Earthquake,PGA

1. Introduction

Kathmandu, the capital city of Nepal, is situated amidst the landscapes of the Himalayas and holds significant geological and seismic importance. Being located in an area of seismic activity due to the collision of the Indian and Eurasian tectonic plates, Kathmandu faces the risk of earthquakes with varying intensities that can potentially cause severe damage to its infrastructure, historical monuments, and economy. Nepal has a history of experiencing major earthquakes every 80–100 years measuring above 7 on the moment magnitude (M_w) scale [1]. The Nepal-Bihar earthquake in 1934 (magnitude 8.3), the Udayapur earthquake in 1988 (magnitude 6.5), and more recently the Gorkha earthquake in 2015 ($M_w = 7.8$), have caused severe structural damage in Kathmandu and the surrounding area[2]. One such tragic occurrence (called Gorkha Earthquake 2015) struck on April 25, 2015, with a moment magnitude (M_w) of 7.8 and its epicentre 80 kilometres northwest of Kathmandu. The study of site-specific hazard analysis has been regarded as crucial since the Kathmandu valley is home to several architectural marvels and is densely populated, with a population of over 3.1 million (as of the census of 2021).

Site effects in earthquakes relate to how local soil and geological characteristics may either amplify or attenuate ground shaking during an earthquake, affecting the extent of damage in a specific location. Site effects are crucial in characterizing seismic ground motion because they can significantly amplify seismic motions at the last moment, just before they reach the ground's surface or the basement of man-made structures. Given that the layers above bedrock can alter ground motion characteristics, such as amplitude, frequency content, and duration of earthquake motion [3], understanding the impact of local soil conditions on

amplifying seismic wave motion is crucial for the Kathmandu Valley.

Numerous local site effects have been observed in historical earthquakes around the world. The significance of local site effects became evident following the Michoacán earthquake in 1985, with its epicentre located in Michoacán, approximately 320 km from Mexico City. Similarly, The local site effects on earthquake damage have been shown in previous earthquakes like the Northridge earthquake (1994), Kobe earthquake (1995), Bhuj earthquake (2001), Kashmir earthquake (2005), Sichuan earthquake (2008), Chile earthquake (1985), and the Haiti earthquake (2010) [4]. Dixit et al. (2000) [1] have concluded that the Kathmandu valley is characterized by substantial local site effects based on the degree of damage inflicted in the valley during previous earthquakes, notably the 1934 Bihar-Nepal earthquake.

2. Geology and Seismicity of Study Area

The Kathmandu valley used to be believed to be a lake. It is thought to be surrounded by more than 550 meters of fluvial and lacustrine deposits that date from the late Pliocene to the Pleistocene[5]. The typical lacustrine deposits found in the Kathmandu valley have drawn several geoscientists from around the globe[6]. Figure 1 illustrates the Kathmandu valley's geological background with various formations. Kathmandu valley, located in Nepal's Lesser Himalayan zone, is a part of the broader Himalayan Mountain range. The valley is close to the Main Central Thrust (MCT), a significant geological fault that marks the boundary between the Lesser Himalayas and the Greater Himalayas. The spatial distribution of earthquakes shows a correlation with major faults, particularly the Main Central Thrust (MCT)[7]. The MCT and tectonic collision between the Indian and Eurasian

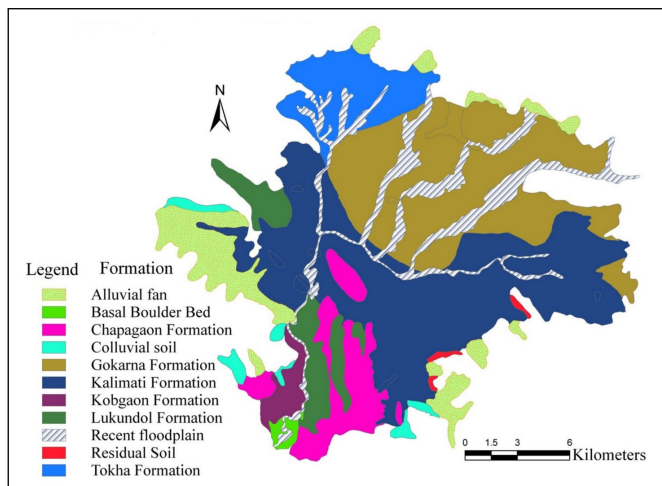


Figure 1: geological map of Kathmandu valley (Source: Department of Geology and Mines)

plates contribute to the uplift of the Himalayan Mountain range, making the valley susceptible to seismic activity and ongoing geological changes.

3. Methodology

3.1 Data Collection

The Standard Penetration Tests (SPT) conducted at different locations of Kathmandu valley were obtained from site investigation reports and through journals, reports, engineering consultancies, and Kathmandu Upatyaka Khanepani Limited (KUKL). The borehole logs included visual classification of soil, the Unified Soil Classification System (USCS), and records of SPT values at every depth interval of 1.5m. For the study, Borehole log data from 32 different locations drilled at 8-30m were assessed. The spatial distribution of the Borehole log is illustrated in figure 2.

In the absence of geophysical experiments, the shear wave velocity was approximated. Several empirical correlations relate the shear wave velocity (V_s) of different soil layers to the SPT-N value. The Kathmandu valley is primarily made up of unconsolidated Pleistocene and Holocene (recent) sediments, like fluvial and lacustrine deposits, that are resting on a sequence of metamorphic and partially metamorphic pre-Tertiary bedrock [8]. (Ohta & Goto, 1978) [9] proposed the shear wave velocity based on geology (i.e., based on deposition & age) and uncorrected SPT for all soils is represented by equation 1.

$$V_s = 134.2N^{0.27} \quad (1)$$

(Kawan et al., 2022) [10] also employed equation (1) to compute shear wave velocity and subsequently averaged them using a relationship based on depth. Moreover, equation (1) can provide a reliable estimate of the shear wave velocity of a soil profile with an SPT value due to its correlation coefficient of 0.784 and likely error of 24.2%. Due to the absence of the Unit Weight of soil at each layer of the borehole log from the lab test, the Unit weight of soil strata is attained with Average soil engineering properties according to USCS classification as per (Krahenbuhl and Wagner, 1983) [11].

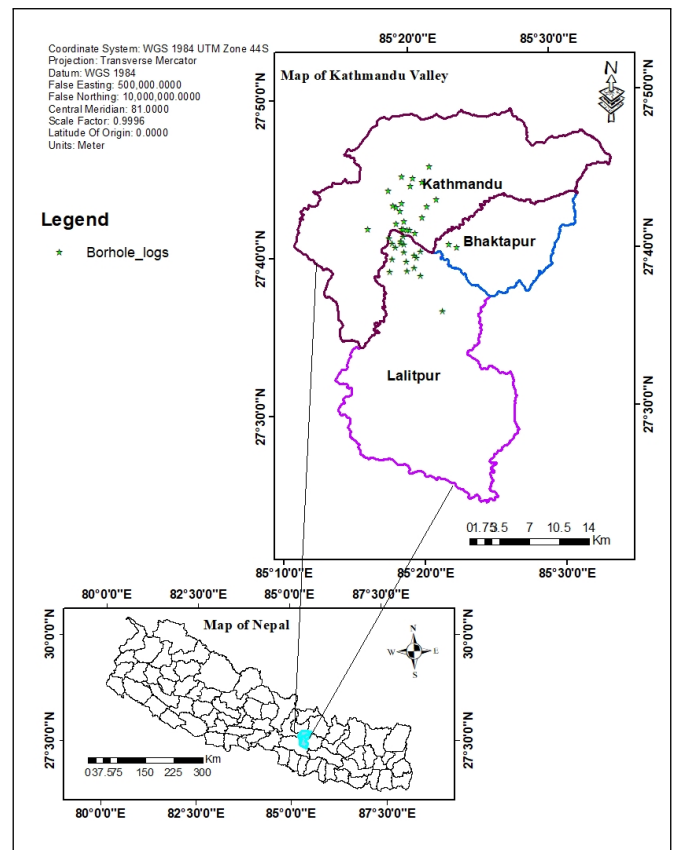


Figure 2: Study area map and borehole log location

3.2 Hyperbolic model

Using the DEEPSOIL [12], one-dimensional non-linear ground response assessments have been performed. The non-linear time domain analysis represents the cyclic behaviour of soil. To accurately model ground response using the nonlinear methodology in the time domain, the equation of motion must be solved for each small-time increment represented by equation (2).

$$M\ddot{u} + C\dot{u} + Ku = F(t) \quad (2)$$

where M is the mass matrix, C is the damping matrix, K is the stiffness matrix, u is the displacement vector, \ddot{u} is the acceleration vector, \dot{u} is the velocity vector, and $F(t)$ is the force vector applied at each time [3].

The initial backbone curve for the first loading cycle is described by the hyperbolic stress-strain model, which was initially developed by Kondner and Zelasko in 1963 [13] and then revised by Matasovic and Vucetic (1993) [14] and Hashash and Park (2001) [15]. Modelling the soil stiffness degradation with the developing pore water pressure as the parameter results in the stress-strain behaviour in the succeeding cycles. The DEEPSOIL 7.0 [12] algorithm uses the curve fitting approach created by Hashash (2009) [16], commonly known as MRDF-UIUC, to perform non-linear non-Masing analysis. This procedure altered the Masing (1926) [17] and extended Masing rules.

3.3 Modulus Reduction and Damping curves

Modulus reduction curves and damping ratio curves have been selected based on different types of soil classifications.

Table 1: Earthquake motion acceleration Time History Data [18]

S.N	Earthquake Motion	Date	Recording Station	Epicenter to station distance	Magnitude	PGA (g)
1	Gorkha Earthquake	2015-04-25	Kritipur Municipality	77 Km	7.8 Mw	0.156g
2	Chi-Chi Earthquake	199-09-21	Taichung, Taiwan	24.8 Km	7.6 Mw	0.18g
3	Kobe Earthquake	1995-01-17	JMA Station	0.6 Km	6.9 Mw	0.82g
4	Lima-Gilroy Earthquake	1989-10-17	Gilroy Array Station	12.2 Km	6.9 Mw	0.17g
5	Aftershock of Gorkha Earthquake	2015-04-25	kritipur Municipality	7.14 Km	5 Mb	0.055g

In the absence of site-specific modulus reduction and damping curves, standard curves proposed by Vucetic and Dobry (1991)[19], and Seed and Idriss (1970)[20] for clay and sand are used respectively. A plot of the modulus reduction and damping ratio curve adopted in the study is shown in figure 3 and 4.

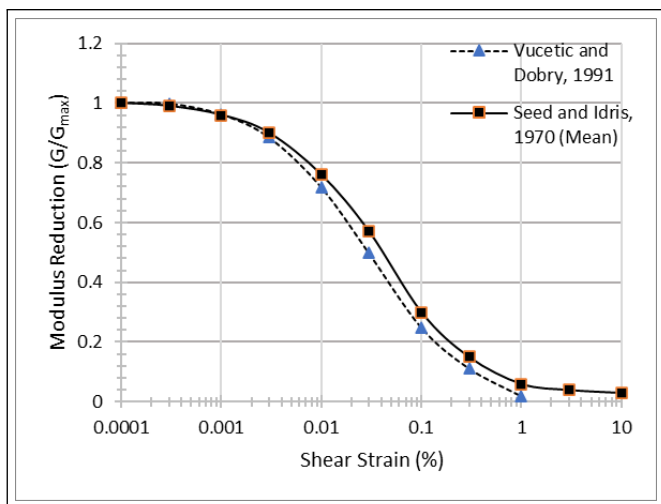


Figure 3: Modulus Reduction curve[19], [20]

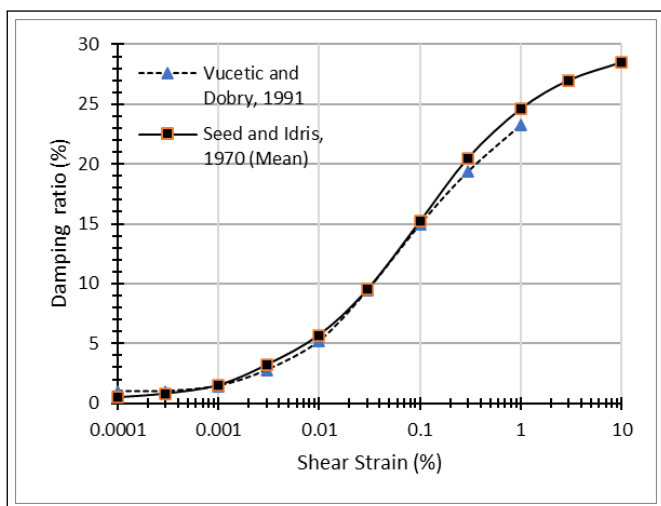


Figure 4: Damping ratio curve[19], [20]

3.4 Input Motion

The ground response study involves producing or obtaining an acceleration time history that corresponds to the highest dynamic loading estimated at the site of interest. For this study, five different earthquake motions, the Gorkha Earthquake (2015) motion, the Kobe Earthquake (1995)

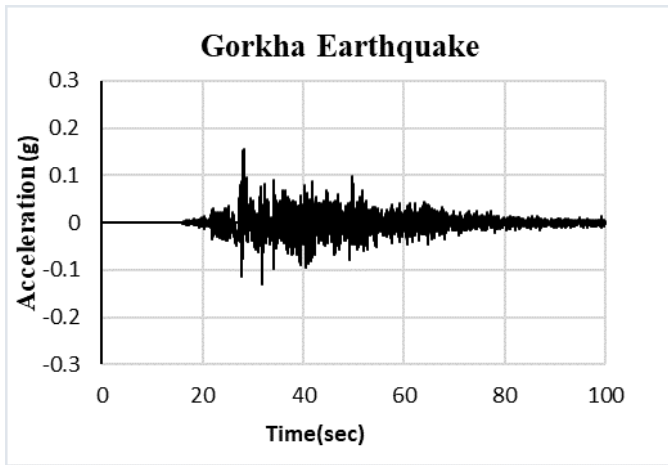
motion, the Loma-Gilroy Earthquake(1989) motion, the Chi-Chi Earthquake (1999) motion and the Aftershock of Gorkha Earthquake (2015) motion are selected. These selections encompass a range of seismic intensities recorded at various stations, as outlined in table 1.

With a PGA of 0.156g, the Gorkha earthquake motion serves as a benchmark for recent seismic activity in Nepal, and its aftershocks that has a lower PGA of 0.055g help in the investigation of residual ground shaking impacts. The Chi-Chi earthquake motions and Loma-Gilroy earthquake motions, with PGAs of 0.18g and 0.17g, respectively, offer insights into regions with more moderate seismic danger, whereas the Kobe earthquake, with a high PGA of 0.82g, indicates severe seismic circumstances. Figure 5 displays the acceleration time history of five different earthquake motions, showcasing differing seismic intensities, from the lowest PGA to the highest PGA.

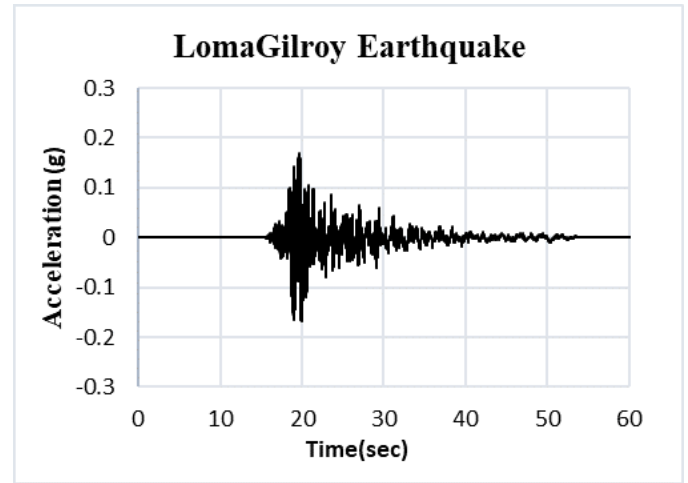
4. Result and discussion

The study presents the variation in AF across different input earthquake motions, revealing the ground response characteristics at various locations of the Kathmandu valley as shown in Table 2. These AF offer insight into how seismic waves are amplified or attenuated during different earthquake motions, emphasizing the significance of geological factors and earthquake characteristics in shaping ground response.

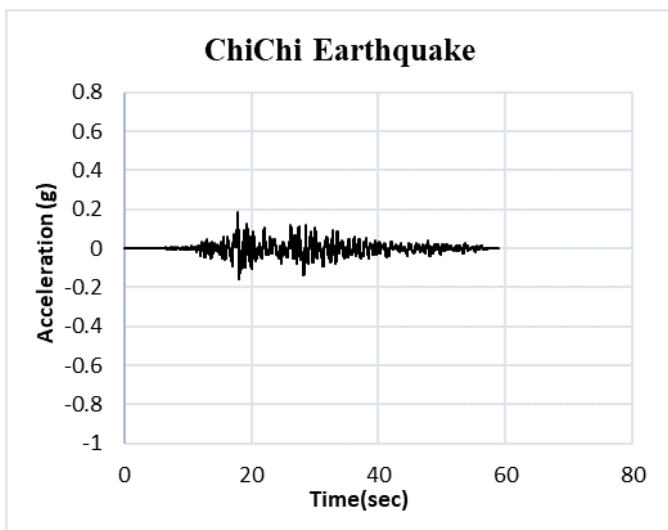
Site response is complicated, as seen by the wide variation in AF across different locations and earthquake motions. This suggests that the soil in Kathmandu has an amplifying character. The analysis of AF reveals a notable similarity between the Gorkha earthquake(2015) motion and the Loma-Gilroy earthquake(1989) motion. The amplification factor observed during the Chi-chi earthquake is moderate. However, it is interesting to observe that higher amplification factors are associated with the aftershock of the Gorkha Earthquake, while lower amplification factors tend to be observed during the Kobe earthquake. Kumar et al.(2015) [21] studied the relationship between Peak Horizontal Acceleration (PHA) and amplification factors. Kumar et al.(2015) [21] study revealed that the rate of change in amplification factor varies significantly with different Peak Horizontal Acceleration (PHA) levels. Specifically, the rate of change is reported as very high for PHA values less than 0.08g, intermediate for PHA values ranging between 0.08g and 0.22g, and low for PHA values exceeding 0.22g [21]. The observation of higher amplification factors (AF) corresponding to very low values of peak ground acceleration (PGA), as exemplified by the case of aftershocks with a PGA of 0.055g, finds validation in prior research of Kumar et. al(2015)[21].



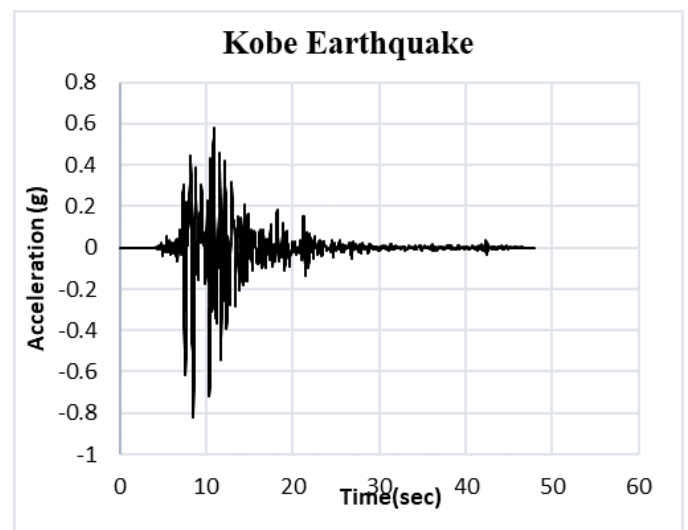
(a)



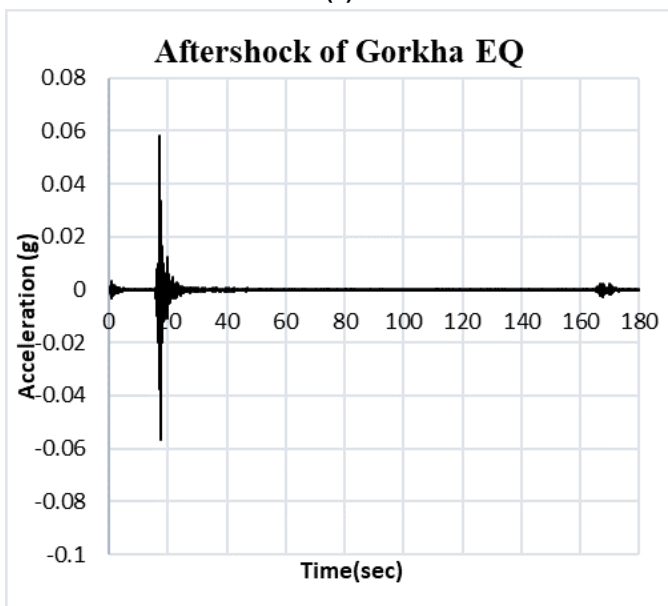
(b)



(c)



(d)



(e)

Figure 5: a,b,c,d,e: Variation in Peak Ground Acceleration (PGA) across five earthquake motion records, highlighting seismic intensity differences

Table 2: Amplification factor in various locations in Kathmandu valley across different earthquake Motions

S.N	Notation	Location	Gorkha	Chi-Chi	Aftershock	Kobe	Lima Gilroy
1	BH-K1	Thapathali	1.212	1.184	1.898	0.423	1.350
2	BH-K2	Anamnagar	1.217	1.168	1.522	0.416	1.321
3	BH-K3	New Baneswor	1.395	1.336	1.813	0.397	1.211
4	BH-K4	Balaju	1.904	1.264	2.156	0.796	2.057
5	BH-K5	Maharajung	1.729	1.350	2.139	0.803	1.848
6	BH-K6	Gongabu	1.530	1.400	1.992	0.543	1.414
7	BH-K7	Budhanilkantha	1.814	1.242	2.085	0.907	1.958
8	BH-K8	Basbari	1.812	1.207	1.827	0.824	1.829
9	BH-K9	Basundhara	1.780	1.229	2.098	0.911	1.909
10	BH-K10	Boudha	1.711	1.382	2.158	0.858	1.738
11	BH-K11	Thamel	1.303	1.191	1.430	0.428	1.449
12	BH-K12	Babarmal	1.119	1.039	1.298	0.342	1.145
13	BH-K13	Sorakhutte	1.753	1.415	2.260	0.701	1.896
14	BH-K14	Lazimpat	1.357	1.440	1.627	0.527	1.364
15	BH-K15	Durbaramarg	1.560	1.320	2.097	0.747	1.689
16	BH-K16	Battisputali	1.712	1.348	2.182	0.810	1.762
17	BH-K17	Putalisadak	0.905	0.833	1.103	0.250	0.976
18	BH-K18	Maitighar	1.112	1.169	1.375	0.379	1.201
19	BH-K19	Chabahil	1.782	1.208	1.956	0.934	1.913
20	BH-L1	Imadol	1.455	1.404	1.773	0.530	1.378
21	BH-L2	Pulchowk	1.506	1.281	1.813	0.766	1.480
22	BH-L3	Kupandol	1.125	1.030	1.409	0.353	1.196
23	BH-L4	Kumaripati	1.561	1.163	1.502	1.001	1.754
24	BH-L5	Balkumari	1.137	1.048	1.315	0.385	1.300
25	BH-L6	Sanepa	1.151	1.231	1.291	0.467	1.166
26	BH-L7	Hariharbhawan	0.832	0.681	0.958	0.205	0.770
27	BH-L8	Gwarko	0.998	0.946	1.184	0.333	1.090
28	BH-L9	Hatiban	1.323	1.311	1.711	0.462	1.331
29	BH-L10	Patan	1.520	1.301	2.089	0.509	1.405
30	BH-L11	Jawalkhel	1.451	1.371	1.744	0.542	1.319
31	BH-B1	Chardobato	1.211	1.201	1.666	0.427	1.273
32	BH-B2	Gattaghar	1.058	0.958	1.264	0.334	1.115

The amplification observed is not solely due to the characteristics of the earthquake but also reflects the nonlinearity of the soil response[21]. In nonlinear soil behaviour, soil undergoes changes in stiffness and damping under varying levels of stress, leading to different amplification effects for different ground motion intensities. This is further validated by the study of (Romero, 2001)[22]. As reported by (Romero, 2001)[22], during the 1989 Loma Prieta earthquake and the 1985 Michaoacan earthquake, substantial amplifications related to low-amplitude ground movements were observed.

Similarly, the extreme case of high input Peak Ground Acceleration (PGA) (as of the Kobe earthquake motion) showed a significant reduction in AF, with a range of 0.205 to 1.001, indicating a reduced amplification effect compared to lower input PGA earthquake motion. Large accelerations are a feature of immense strains[22]. The extremely high damping ratio of the soil determines how it responds to huge stresses. As a result, the ground motion will have less amplification factor during high acceleration than the input motions with low acceleration[21] [22]. The variation of AF based on different input PGA of five different earthquake motions is shown in figure 6 considering only three borehole log locations of Kathmandu valley.

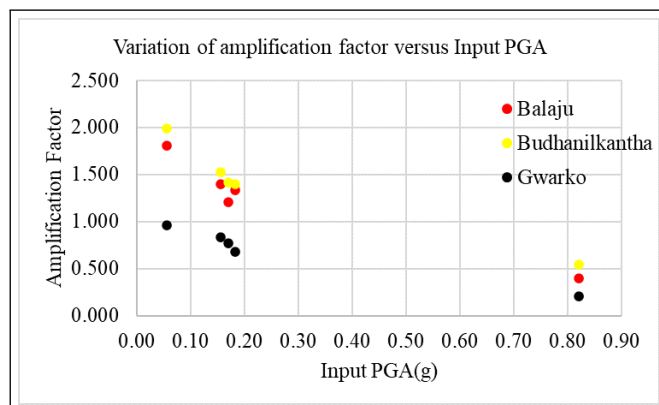


Figure 6: Variation of AF with different earthquake motions' PGA

Also, from the analysis it is found that the Balaju (BH-K4) exhibited the highest amplification factor during the Gorkha earthquake. The amplification factor from Loma Gilroy earthquake motion and the Aftershocks of the Gorkha Earthquake is also higher. This observation aligns with the findings of Hazarika et al.(2016)[23], who identified Balaju as one of the areas in the Kathmandu valley with concentrated damage during the Gorkha earthquake.

5. Conclusion

Using the DEEPSOIL V7[12] non-linear one-dimensional analysis approach, this study investigated the ground amplification factor of soil deposits in the Kathmandu valley. Through the analysis, five distinct earthquake motions were employed to illustrate ground motion across diverse soil profiles in various locations within the valley. Local geology emerged as a crucial factor influencing ground amplification or attenuation during seismic events. The observed amplification factors for the Gorkha earthquake motion and its aftershocks surpassed two times, indicating significant variability in amplification within the Kathmandu valley. This underscores the complexity of ground motion amplification in the region.

This study aims to assess how soil response varies depending on the input motion, utilizing data from five distinct earthquake motions. As per the findings of this study, soil layers experiencing input motion with lower PGA values tend to display a higher AF compared to similar soil columns exposed to input motion with higher PGA values. These observations align with existing literature on the subject.

References

- [1] A Dixit, L Dwelley-Samant, Mahesh Nakarmi, Shiva B Pradhanang, and B Tucker. The kathmandu valley earthquake risk management project: an evaluation. *Asia Disaster Preparedness Centre: <http://www.iitk.ac.in/nicee/wceel/article/0788.pdf>*, 2000.
- [2] Tilak Bahadur Gaha, Bikram Bhusal, Satish Paudel, and Shubheksha Saru. Investigation of ground response analysis for kathmandu valley: a case study of gorkha earthquake. *Arabian Journal of Geosciences*, 15(15):1354, 2022.
- [3] Steven Lawrence Kramer. *Geotechnical earthquake engineering*. Pearson Education India, 1996.
- [4] Effects of surface geology and topography on the damage severity during the 2015 nepal gorkha earthquake. *Lowland Technology International*, 18(4, March):269–282, 2017.
- [5] Mitsuo Yoshida. Neogene to quaternary lacustrine sediments in the kathmandu valley, nepal. *Journal of Nepal Geological Society, Special Issue*, 4:73–100, 1984.
- [6] Youb Raj Paudyal, Ryuichi Yatabe, Netra Prakash Bhandary, and Ranjan Kumar Dahal. Basement topography of the kathmandu basin using microtremor observation. *Journal of Asian Earth Sciences*, 62:627–637, 2013.
- [7] Dilli Ram Thapa. Seismicity of nepal and the surrounding region. *Bulletin of the Department of Geology*, pages 83–86, 2018.
- [8] Mithila Verma, RJ Singh, and BK Bansal. Soft sediments and damage pattern: a few case studies from large indian earthquakes vis-a-vis seismic risk evaluation. *Natural hazards*, 74:1829–1851, 2014.
- [9] Yutaka Ohta and Noritoshi Goto. Empirical shear wave velocity equations in terms of characteristic soil indexes. *Earthquake engineering & structural dynamics*, 6(2):167–187, 1978.
- [10] Chandra Kiran Kawan, Prem Nath Maskey, and Gokarna Bahadur Motra. A study of local soil effect on the earthquake ground motion in bhaktapur city, nepal using equivalent linear and non-linear analysis. *Iranian Journal of Science and Technology, Transactions of Civil Engineering*, 46(6):4481–4498, 2022.
- [11] J Krahenbuhl and A Wagner. Survey, design, and construction of trail suspension bridges for remote areas, skat. *Swiss Center for Appropriate Technology in St. Gallen, Switzerland*, 1983.
- [12] YMA Hashash, MI Musgrove, JA Harmon, O Ilhan, G Xing, O Numanoglu, DR Groholski, CA Phillips, and D Park. Deepsoil 7.0, user manual. *Urbana, IL, Board of Trustees of University of Illinois at Urbana-Champaign*, (2020):1–170, 2020.
- [13] Robert L Kondner. A hyperbolic stressstrain formulation for sands. In *Proc. 2nd Pan-American Conf. on SMFE*, volume 1, pages 289–324, 1963.
- [14] Neven Matasovic and Mladen Vucetic. Cyclic characterization of liquefiable sands. *Journal of Geotechnical Engineering*, 119:1805–1822, 11 1993.
- [15] Youssef M.A. Hashash and Duhee Park. Non-linear one-dimensional seismic ground motion propagation in the mississippi embayment. *Engineering Geology*, 62(1):185–206, 2001. Earthquake hazard evaluation in the Central United States.
- [16] Youssef Hashash, Camilo Phillips, and David R Groholski. Recent advances in non-linear site response analysis. 2010.
- [17] Georg MASING. Eigenspannungen und verfestigung beim messing. In *Proceedings, second international congress of applied mechanics*, pages 332–335, 1926.
- [18] Center for engineering strong motion data, 2024-03-16.
- [19] Mladen Vucetic and Ricardo Dobry. Effect of soil plasticity on cyclic response. *Journal of geotechnical engineering*, 117(1):89–107, 1991.
- [20] Harry Bolton Seed. Soil moduli and damping factors for dynamic response analyses. *Reoprt*, pages EERC–70, 1970.
- [21] Abhishek Kumar, NH Harinarayan, and Olympa Baro. High amplification factor for low amplitude ground motion: assessment for delhi. *Disaster Adv*, 8(12):1–11, 2015.
- [22] Salome M Romero. *Ground motion amplification of soils in the upper Mississippi embayment*. Georgia Institute of Technology, 2001.
- [23] H Hazarika, NP Bhandary, Y Kajita, K Kasama, K Tsukahara, and RK Pokharel. The 2015 nepal gorkha earthquake: An overview of the damage, lessons learned and challenges. *lowland technology international*, 18(2, Sep):119–128, 2016.